Predicting Hemispheric Dominance for Language Production in Healthy Individuals Using Support Vector Machine

Laure Zago [iD],[1,2,3]* **Pierre-Yves Hervé,**[1,2,3] **Robin Genuer,**[4,5]
Alexandre Laurent,[1,2,3] **Bernard Mazoyer,**[1,2,3]
Nathalie Tzourio-Mazoyer,[1,2,3] **and Marc Joliot**[1,2,3]

[1]*Université de Bordeaux, Institut des Maladies Neurodégéneratives, UMR 5293,*
Groupe d'Imagerie Neurofonctionnelle, F-33000 Bordeaux, France
[2]*CNRS, Institut des Maladies Neurodégéneratives, UMR 5293,*
Groupe d'Imagerie Neurofonctionnelle, F-33000 Bordeaux, France
[3]*CEA, Institut des Maladies Neurodégéneratives, UMR 5293,*
Groupe d'Imagerie Neurofonctionnelle, F-33000 Bordeaux, France
[4]*Université de Bordeaux, ISPED, Centre INSERM U-1219, F-33000 Bordeaux, France*
[5]*INSERM, ISPED, Centre INSERM U-1219, F-33000 Bordeaux, France*

◆━━━━━━━━━━━━━━━━◆

Abstract: We used a Support Vector Machine (SVM) classifier to assess hemispheric pattern of language dominance of 47 individuals categorized as non-typical for language from their hemispheric functional laterality index (HFLI) measured on a sentence *minus* word-list production fMRI-BOLD contrast map. The SVM classifier was trained at discriminating between *Dominant* and *Non-Dominant* hemispheric language production activation pattern on a group of 250 participants previously identified as Typicals (HFLI strongly leftward). Then, SVM was applied to each hemispheric language activation pattern of 47 non-typical individuals. The results showed that at least one hemisphere (left or right) was found to be *Dominant* in every, except 3 individuals, indicating that the "dominant" type of functional organization is the most frequent in non-typicals. Specifically, left hemisphere dominance was predicted in all non-typical right-handers (RH) and in 57.4% of non-typical left-handers (LH). When both hemisphere classifications were jointly considered, four types of brain patterns were observed. The most often predicted pattern (51%) was left-dominant (*Dominant* left-hemisphere and *Non-Dominant* right-hemisphere), followed by right-dominant (23%, *Dominant* right-hemisphere and *Non-Dominant* left-hemisphere) and co-dominant (19%, 2 *Dominant* hemispheres) patterns. Co-non-dominant was rare (6%, 2 *Non-Dominant* hemispheres), but was normal variants of hemispheric specialization. In RH, only left-dominant (72%) and co-dominant patterns were detected, while for LH, all types were found, although with different occurrences. Among

---

the 10 LH with a strong rightward HFLI, 8 had a right-dominant brain pattern. Whole-brain analysis of the right-dominant pattern group confirmed that it exhibited a functional organization strictly mirroring that of left-dominant pattern group. *Hum Brain Mapp* 38:5871–5889, 2017. © 2017 **W**iley Periodicals, Inc.

◆ ━━━━━━━━━━━━━━━━━━━━━━━━━━━━━━━ ◆

INTRODUCTION

In a previous functional magnetic resonance imaging (fMRI) study [Mazoyer et al., 2014], we applied a Gaussian mixture modeling to the distribution of an hemispheric functional lateralization index (HFLI, [Wilke and Schmithorst, 2006] for a language production task in a large sample of 297 healthy individuals enriched in left-handers (LH). We so identified three groups having distinct language production lateralization, namely, typical leftward language lateralization (Typical, $N = 250$), lack of lateralization (Ambilateral, $N = 37$), and atypical strong rightward lateralization (Strong-atypical, $N = 10$). In a subsequent study [Tzourio-Mazoyer et al., 2016], we used an intrinsic connectivity-based homotopic areas atlas (AICHA atlas, [Joliot et al., 2015] for characterizing the regional patterns of activation asymmetry of the Ambilateral and Strong-atypical groups, and compare them to that of Typical group. Investigating the effect of handedness on the regional profiles of asymmetry, we showed that the right-hander (RH) Ambilaterals, although having a weak leftward asymmetry, had a regional profile of asymmetry comparable to that of Typicals, testifying for a typical language organization. By contrast, LH Ambilaterals exhibited a profile different from that of either Typicals or Strong-Atypicals groups: for this group, it was indeed not possible to infer on sole basis of the regional asymmetry pattern which hemisphere was dominant, if any. One hypothesis for this phenomenon could be that the LH Ambilateral group actually gathered individuals having different patterns of hemispheric dominance for language: testing this hypothesis would clearly require an individual assessment of hemispheric dominance.

Asymmetry or laterality indices measured during functional MRI language tasks have been used to assess hemispheric lateralization of language in healthy individuals [Baciu et al., 2005a; Seghier et al., 2010] or neurosurgical patients [Baciu et al., 2005b]. Although these indices have shown a good concordance with Wada testing used for assessing language lateralization in patients prior to brain surgery [Binder, 2011; Dym et al., 2011 for reviews], there are still uncertainties when such hemispheric dominance is assessed in case of low asymmetry measured from functional imaging of language tasks [Benke et al., 2006]. Moreover, the question of the existence of hemispheric dominance in healthy individuals showing a lack of lateralization such as in Ambilaterals, is in line with a report on 445 epileptic patients that evidenced two types of bilateral language dominance: in a small number of patients, anesthesia of either hemisphere produced speech arrest, suggesting two dominant hemispheres, whereas in another very rare subgroup, there was no speech arrest after either carotid injection, indicating lack of a dominant hemisphere [Möddel et al., 2009]. Whether both such types of language hemispheric dominance also exist in healthy participants remains an open issue. In a recent review, we proposed, that patterns of plasticity or recovery observed in epileptic patients should in theory be observable in healthy individuals, although in rare cases only [Tzourio-Mazoyer et al., 2017]. Interestingly, Hécaen has previously reported in a large sample of LH more frequent complete language recovery after lesion of either hemisphere, which led him to propose the concept of ambilaterality [Hécaen et al., 1981]. However, the particular neural support for ambilaterality remains unknown and could correspond to bilateral either dominant or non-dominant hemispheres. Because we previously demonstrated that RH Ambilaterals exhibited a typical leftward asymmetrical regional pattern [Tzourio-Mazoyer et al., 2016], there is also the possibility that these individuals have a global weak cerebral asymmetry but still left hemisphere dominance for language. To answer these questions, one needs to be able to categorize for a given individual the pattern of language activation in each of his/her hemisphere independently, rather than comparing his/her left-right hemispheric asymmetries. In other words, while HFLI provides global information on which hemisphere has the stronger activation during language tasks, it does not provide any information on the specific hemispheric regional pattern of activation, what is the core of the neural bases of hemispheric dominance for language.

In the same vein, we have previously shown that the Strong-atypical group exhibited a mirrored image of the regional asymmetries found in the Typical group [Tzourio-Mazoyer et al., 2016]. Although such a regional profile of asymmetries suggests that these individuals are good candidates for right hemispheric dominance for language [Tzourio-Mazoyer et al., 2017], a phenomenon also reported by Drane with cortical stimulation [Drane et al., 2012], one may question whether such regional asymmetries really correspond to a pattern specific to a right dominant hemisphere for language in each Strong-atypical individual. Besides, the status of the left hemisphere pattern of these individuals remains open as hemispheric asymmetry indices do not provide a hemispheric categorization.

The primary aim of the present study was thus to categorize the activation pattern of each hemisphere of non-typical language lateralized individuals, such as Ambilaterals and Strong-atypicals, as previously identified in the Mazoyer et al.' study [Mazoyer et al., 2014]. We used a Support Vector Machine (SVM) approach [Noble, 2006] for categorizing each hemisphere as either *dominant* or *non-dominant* based on its respective activation map during language task. This approach requires a learning phase during which the SVM will learn to recognize how a *dominant* or a *non-dominant* hemispheric patterns looks like for individuals typically lateralized for language: for this phase, we used the large sample of 250 individuals from the BIL&GIN database [Mazoyer et al., 2015] that were declared strongly leftward lateralized for language from a previous analysis [Mazoyer et al., 2014]. We then applied the SVM to the group of 47 individuals known to be non-typical for language for deciding whether each of their hemispheres was *dominant* or *non-dominant*. This allowed to report on occurrences of the four possible outcomes of this procedure, namely (1) a left-dominant brain pattern when the left hemisphere is classified as *Dominant* and the right hemisphere as *Non-Dominant*; (2) a right-dominant brain pattern when the right hemisphere is classified as *Dominant* and the left one as *Non-Dominant*; (3) a co-dominant brain pattern when both hemispheres are classified as *Dominant*; (4) a co-non-dominant brain pattern when both hemispheres are classified as *Non-Dominant*. We then investigated differences in regional brain activation patterns between the four categories to refine our understanding of the variability of functional brain networks in individuals atypical for language lateralization.

MATERIALS AND METHODS

Participants

The sample of 297 participants has been fully described elsewhere [Mazoyer et al., 2014] and is part of the BIL&GIN database [Mazoyer et al., 2015]. Briefly, we recruited a sample of 297 individuals, balanced for handedness and sex (144 RH, including 72 women; 153 LH, including 73 women). Note that this sample is not representative of the general population, as it was deliberately enriched in LH aiming at a 50/50 ratio.

Handedness was self-reported by the participants and their manual lateralization strength quantified using the Edinburgh inventory [Oldfield, 1971]. Sample mean age was 25.3 years (S.D. = 6.4 years, range: 18–57 years) and sample mean level of education was 15.6 years ± 2.3 years (range: 11–20 years) corresponding to almost 5 years of education after the French baccalaureate. A local ethics committee (CCPRB Basse-Normandie) approved the experimental protocol. Participants gave their informed written consent, and received an allowance for their participation. All participants were free of brain abnormality as assessed by an inspection of their structural T1-MRI scan by a neuroradiologist.

Sentence and Word List Production Tasks

We evaluated language production neural networks using a slow event-related functional MRI of covert production of sentences and covert recitation of a list of overlearned words.

Subjects were presented white line drawing pictures on a black screen which were either cartoons depicting a scene involving characters, or a scrambled version of these pictures. Right after the presentation of a picture, subjects had to covertly generate either a sentence when they saw a cartoon or to enunciate the ordered list of the months of the year when they saw a scrambled picture.

Subjects were instructed to generate sentences each having the same structure, starting with a subject and a complement followed by a verb describing the action taking place, ending with another complement of place. During this generation period, participants had to fixate a white-cross displayed at the center of the screen and to press the pad with their index finger when they had finished covertly enouncing the sentence. The list of word recitation consisted in to covertly enunciate the ordered list of months of the year and to press the pad when finished.

Each trial was 18-sec long, the time limit for response being 9 sec including the 1-sec picture display. A 12-sec presentation of a fixation crosshair preceded and followed the first and last trial of each run. This slow event-related experimental paradigm randomly alternated 10 trials of sentence generation with 10 trials of recitation of a list of months. Overall, the fMRI run lasted 6 min 24 sec, response time in reciting each list of words or generating each sentence being recorded using a fiber optic pad.

Structural and Functional Image Acquisition and Processing

Imaging was performed on a Philips Achieva 3Tesla MRI scanner. The structural MRI protocol consisted of a localizer scan, a high resolution 3D T1-weighted volume acquisition (TR = 20 ms; TE = 4.6 ms; flip angle = 10 deg.; inversion time = 800 ms; turbo field echo factor = 65; sense factor = 2; matrix size = 256 × 256 × 180; 1 mm^3 isotropic voxel size) and a T2*-weighted multi-slice acquisition (T2*-FFE sequence, TR = 3,500 ms; TE = 35 ms; flip angle = 90 deg.; sense factor = 2; 70 axial slices; 2 × 2 × 2 mm^3 isotropic voxel size). Functional volumes were acquired with a T2*-weighted echo planar imaging acquisition (192 volumes; TR = 2 s; TE = 35 ms; flip angle = 80 deg.; 31 axial slices; 3.75 × 3.75 × 3.75 mm^3 isotropic voxel size) covering the same field of view than the T2*-FFE acquisition.

Image analysis was performed using the SPM5 software (www.fil.ion.ucl.ac.uk/spm). The T1-weighted scans of each participant was normalized to our site-specific template
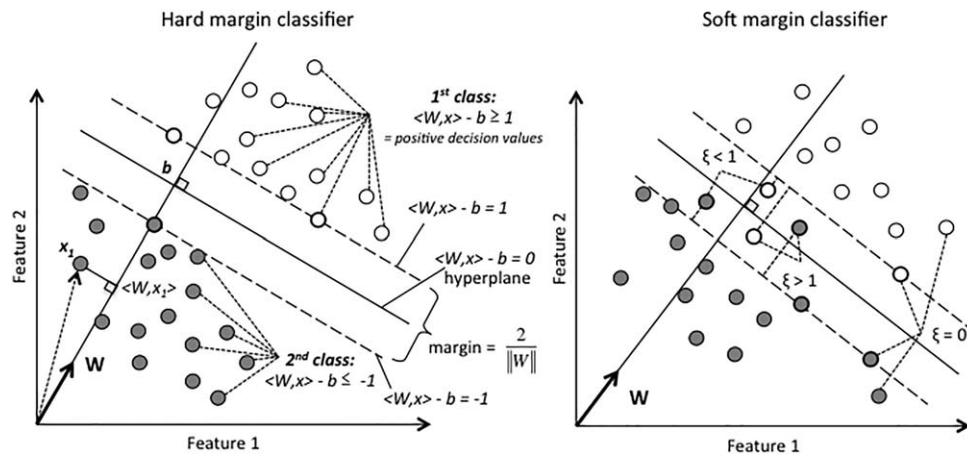
Figure 1.

Schematic of a 2-dimensional hard- (left) and soft- (right) margin Support Vector Machine with two classes to separate. Each observation of the learning set is plotted according to its value on the two features included in the analysis. Class 1 is plotted with open circles, Class 2 with closed circles. The dashed lines represent the margins. Thick circles highlight the support vectors (observations that define the margins). The separating hyper-plane is situated halfway between the two margins. Left: Hard-margin classifier. In this example, all points of the first class have a positive decision value, and all points of Class 2 have a negative decision value. Right: Soft-margin classifier. Note the location of the observation and their corresponding slack value (ξ): 0 if outside the margin, <1 and >1 if located on the right and wrong side of the hyperplane, respectively.

(T1–80 TVS) matching the MNI space, using the SPM5 "segment" procedure with default parameters allowing for segmentation of gray matter, white matter and cerebrospinal fluid components. To correct for motion during the fMRI run, each of the 192 EPI-BOLD scans of each individual was realigned to his first one using a rigid-body registration. The participant EPI-BOLD scans were then rigidly registered to his structural T2*-weighted image, which was itself registered to his T1-weighted scan. The combination of all registration matrices allowed each EPI-BOLD functional scan to be warped into the standard MNI space using a tri-linear interpolation, with subsequent smoothing using a 6-mm full width at half-maximum Gaussian kernel. We applied a general linear modeling approach to local BOLD signal variations, effects of interest being modeled by boxcar functions corresponding to paradigm timing, convolved with the standard SPM hemodynamic temporal response function. We then computed the effect of interest-related individual contrast maps, corresponding to the sentence *minus* list of words production contrast (PROD$_{SENT-LIST}$). Each map was further subdivided in a left and in a right hemispheric contrast maps.

SVM CLASSIFICATION

The basic principle of a SVM classifier is to find the hyper-plane (that is a subspace of dimension $d-1$ in the feature space of dimension d: think to a plane in a 3-dimensional space for example) optimally separating two classes of data (here, hemispheric contrast-maps as *Dominant* or *Non-Dominant*) and to use that hyper-plane for making decision regarding the class a new data should be assigned to. As shown in Figure 1, in a simplistic bi-dimensional feature space example, the hyper-plane is defined by the equation $<W, x> - b = 0$, with $<W, x>$ the scalar product of W (vector orthogonal to the hyper-plane) named feature weight, and a point in space (the projection of x onto W) and b the intercept term. Note that the margin size is inversely proportional to the norm of W. Based on this hyper-plane, a decision value (DV) is computed over all features of each hemisphere. Here, a positive DV will code for the *Dominant* class, and a negative DV value will code for the *Non-Dominant* class. Definition of the hyper-plane is achieved by training the SVM classifier thanks to a "learning" set of data for which the classification is a priori known. Once trained, the SVM classifier can then make decision on a "prediction set" of data for which classification is a priori unknown.

Definition of Learning and Prediction Sets

Learning set

It included the 500 hemispheric PROD$_{SENT-LIST}$ contrast-maps of 250 individuals (130 RH, 120 LH) of the sample previously categorized as typically left-lateralized for language. Such categorization was based on the optimal Gaussian mixture model fitting the sample distribution of the HFLI derived from the PROD$_{SENT-LIST}$ individual positive *t*-map [for details, Mazoyer et al., 2014]. The 250 left-

hemispheres were labeled as *Dominant*, and the 250 right-hemispheres as *Non-Dominant*.

Prediction set

It included the 94 hemispheric PROD$_{SENT-LIST}$ contrasts of the remaining 47 individuals of the sample (14 RH and 33 LH), who had been previously categorized as non-typically lateralized for language being either Ambilateral (weak HFLI lateralization) or Strong-atypical (rightward HFLI lateralization) in Mazoyer et al. [2014] study.

Summary and Rationale of SVM Procedure

We adapted an SVM procedure to the classification of hemispheric contrast-maps as either *Dominant* or *Non-Dominant*. Note that, as recommended by Ambroise and McLachlan [2002], the prediction set plays no role in the feature-selection process that was only based on the learning set. First, we defined a symmetric gray matter analysis mask to overcome anatomical asymmetries, and extracted the voxels within this mask from the PROD$_{SENT-LIST}$ contrasts for each hemisphere. In keeping with machine learning terminology, henceforward, voxels will be referred to as features. We used a soft-margin SVM classifier (see below) to deal with potential classification errors in the learning set because although HFLI allows identifying individuals with strong typical leftward asymmetry, it does not assert that the hemispheric pattern of the left hemisphere is actually a dominant one at the regional level. To base the classification on the most relevant features, we used a recursive feature elimination (RFE) procedure. The accuracy of the classifier was determined with a leave-one-subject-out (LOSO) validation. One of the advantages of the LOSO procedure is that it provides a classification of each individual constituting the learning set. This offers us the unique opportunity to document the range of variability of hemispheric specialization for language in healthy participants, still under-evaluated in typical healthy individuals. Our hypothesis is that within the large sample of individuals constituting the learning set, some rare individuals with particular regional profiles might be evidenced [Price and Friston, 2002].

All these steps are detailed below and illustrated in Figure 2. After completion of this procedure, the classifier was applied to the 94 hemispheres of the prediction set.

We also completed a SVM analysis using a different methodological approach that provides an evaluation of the SVM accuracy. Actually, the LOSO procedure is criticized in terms of the evaluation of the accuracy [Ambroise and McLachlan, 2002] and other methods have been proposed allowing to complete the validation of the machine learning procedure by sampling the population of the learning set in two different groups, one for the learning and one for the validation. However, such methodology does not provide the classification of the individuals of the learning set as the LOSO does. Nevertheless, we completed a fivefold cross-validation procedure described as Supporting Information

to assess the robustness of the SVM procedure with LOSO we applied (see Supporting Information).

Definition of the Symmetrical Analysis Mask and Feature Extraction in the Learning Set

The first step was to define the analysis mask to be used for extracting the features. For this, we computed a symmetric gray matter mask, thereby overcoming gross anatomical asymmetries of the cortical mantle. We did so by averaging the stereotaxic gray matter probability map of the 80-TVS template with its left-right mirror image, and then applying a threshold of 0.2, that corresponds to a 20% or greater probability for a particular voxel to belong to the gray matter tissue class. As SVM was to be applied separately on each hemispheric contrast-maps, only a left hemisphere analysis mask was needed for the feature extraction step. Accordingly, the mask was applied to the raw contrast-map in case of a left hemisphere or to its left-right mirror in case of a right hemisphere. Within this gray matter mask, we retained voxels having a *t*-value larger than 1.96 in at least 50% of the PROD$_{SENT-LIST}$ contrast-maps of the learning set, in either the left or the right hemisphere. We identified 9,901 such voxels. Finally, for each voxel, the distribution of the *t*-values in that voxel across the 500 hemispheres was normalized so as to have zero mean and unit variance.

SVM Classifier

Here, we used a soft-margin classifier refereed as a *v*-classification linear SVM [Schölkopf et al., 2000] (Fig. 1, right) because such classifier is particularly suited for dealing with errors of classification in the learning set. Contrary to hard margin classifiers that compute the hyper-plane with the largest possible margin, (i.e., maximizing the space that segregates the two classes; Fig. 1, left), soft-margin classifiers allow for points of the learning set to lie within the margin, or even on the wrong side of the plane (Fig. 1, right). This provides a solution to classification problems that are not fully linearly separable and/or when the learning set may include a priori classification errors. Soft-margin classification is achieved thanks to a slack variable (ξ), that quantifies the distance between the hyper-plane and the observation in the direction of *W*. ξ value is set at zero if the observation lies on or outside the margin, superior to 0 and inferior to 1 if it is within the margin, but still on the right side of the hyper-plane, and superior to 1 if it is on the wrong side. While hard margin classifiers seek only at minimizing the norm of *W* (and thus maximize the margin), soft-margin classifiers seek both at maximizing the margin size and at minimizing the sum of all slack variables. Here, the *v* parameter ($v \in [0, 1]$), which is the lower and upper bound on the number of examples that are support vectors and that lie on the wrong side of the hyper-plane, respectively [Chen et al., 2005], was set at 0.15. In other word, with such a value, at least 15% of the observations are support vectors
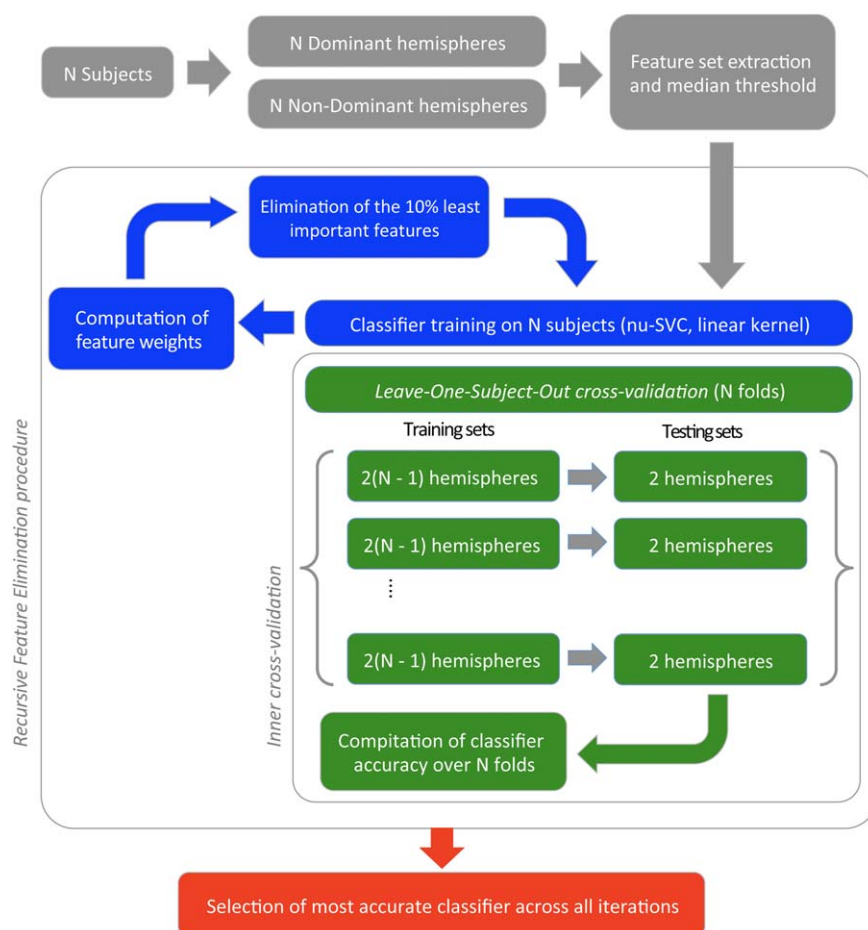
Figure 2.

The same Machine Learning Procedure is applied to either the complete training set, or each fold of the leave-one-subject-out (LOSO) cross validation scheme (in our context, each subject provides two hemispheres, therefore two observations). When applied to the full training set ($N = 250$ Typical participants), the procedure provides a classifier, able to discriminate between Dominant and Non-Dominant hemispheres. The Machine Learning Procedure entails three steps. First, we select the voxels active in more than 50% of the observations in either the Dominant or Non-Dominant hemispheres (gray path). Second, we apply a Recursive Feature Elimination procedure (blue path), in which several SVM classifiers are trained in succession, each time on a smaller feature set. For each iteration, we compute the feature weights, rank them, and eliminate the 10% least important features. For each iteration, we also compute a measure of the relative accuracy of the classifier using inner cross-validation via a LOSO based on 250 folds (green path). For so doing, a classifier is trained on each fold of 249 subjects, and tested on the remaining, unseen subject. Last, we select the classifier exhibiting the best relative accuracy (red path). [Color figure can be viewed at wileyonlinelibrary.com]

(observation that defines the margin, see Fig. 1) and a maximum of 15% of errors can be accommodated.

LOSO Cross-Validation

Throughout the selection of the best classifier (see below RFE procedure) classifier accuracy was estimated using the following LOSO cross-validation procedure: excluding the two hemispheres of a participant from the learning set (as the two are correlated), we trained a classifier over the hemispheres of all remaining participants, and obtained a prediction (either correct or erroneous) for the two excluded hemispheres, to which the classifier was naïve. Iterating this procedure over all subjects of the learning set, one can compute an average success rate. This success rate is here referred to as the classifier's relative accuracy, and is expressed as a percentage. We computed 90% confidence intervals using the 5th and 95th percentiles of the binomial law having as parameter p the classifier's success rate and n the number of classification trials.

RFE Procedure

To base the classification on the most relevant features, a RFE procedure was used [Guyon et al., 2002] for discarding among the initial set of 9,901 features (see above) those containing very little information relevant to the classification problem. To compare the different classifiers from the RFE procedure associated to different number of selected features, their accuracies were estimated using the LOSO procedure. The method is based on the feature weights computed by SVM. As the features were normalized to zero mean and unit variance over the learning set, these weights directly reflect the overall importance of the different features in the classifier's decision, and can be used for selection purposes. Hence, at each step of the LOSO procedure, we trained an SVM classifier and ranked the features based on their weights absolute values. We then eliminated the 10% least important features (with a minimum of 5 features) and reiterated those three steps (SVM training, ranking of features and elimination) and so on. As we started from 9,901 voxels, this entailed performing 75 classifier-training steps. This involved the training of a total of $75 \times 250 = 18,750$ classifiers, each on 498 observations. Among the 75 numbers of features candidates, the one showing the best relative accuracy, as estimated with the LOSO procedure, was retained.

Finally, an SVM classifier, only using the number of most important features previously selected, was built on all 250 participants to be later applied for classification of each hemisphere of the prediction set as either *Dominant* or *Non-Dominant*. At the end, we got selected features set (from which we generate features map), and an SVM classifier that only used those features.

Accuracy of the Procedure

At the end of the RFE procedure, we selected the best number of features based on accuracy values obtained with the complete learning set (i.e., with data from every subject being used for the decision). The accuracy estimate we used for determining the best classifier is therefore biased [Ambroise and McLachlan, 2002] and cannot be used for an estimation of the absolute accuracy of the classifier—although it is fine for choosing between classifiers following the RFE step (a relative comparison). Therefore, to obtain an unbiased accuracy estimate for the whole variable selection procedure, we used an additional external cross-validation: meaning that within each of the 250 cross-validation folds, the initial feature selection with the median threshold, the RFE, the (internal) cross-validation and classifier selection, are performed each time on 498 hemispheres from 249 participants. In other words, we use a nested cross-validation scheme.

The external cross-validation ensures that the estimated accuracy is unbiased, and the internal one allows to compare SVM classifiers built on different feature sets during the RFE procedure. Therefore, across the different folds,

the classifier with the best accuracy can occur after different numbers of iterations. For each of the 250 folds of this nested cross-validation procedure, the winning classifier was tested against the two hemispheres of the subject that has been left out. The average, unbiased, accuracy of our procedure could then be computed on the basis of the 500 predictions performed on the left-out hemispheres by the corresponding winning classifiers.

Implementation

The procedure was implemented with the R statistical software, using the e1071 package for the interface with libSVM, oro.dicom.nifti/Rniftilib for handling the NIfTI image files, and SNOW/Rmpi for parallelizing the computationally expensive nested cross-validation scheme, using a message-passing interface cluster. The analysis was run on the Avakas computer cluster at the Mesocentre de Calcul Intensif d'Aquitaine (MCIA).

Statistical Analyses

Statistical testing of the SVM classification was performed with the JMP09 Pro software package (www.jmp. com, SAS Institute, 2012). Proportions were compared using the Chi-square test. The usual significance level of 0.05 was corrected for multiple comparisons using the Bonferroni–Holm method.

SVM Hemispheric Predictions for the Learning Set

We analyzed the prediction made on each individual of the learning set by the SVM LOSO-RFE classifiers. This cross-validation based on LOSO allows to do the prediction of a given individual without violating the independence between the training and validation set as this given individual is excluded from the training set (see RFE procedure).

SVM Hemispheric Predictions for the Prediction Set

The proportions of left- and right-hemispheres classified as *Dominant* or *Non-Dominant* were calculated for the entire prediction set, as well as separately for RH and LH subjects.

Brain Patterns of Language Dominance

For each individual, classifications of his left- and right-hemisphere were considered together. Four brain patterns were thus possible: (1) a left-dominant brain pattern defined as a *Dominant* left hemisphere and a *Non-Dominant* right hemisphere; (2) a right-dominant brain pattern defined as a *Dominant* right hemisphere and a left one as

Non-Dominant; (3) a co-dominant brain pattern when both hemispheres are classified as *Dominant*; (4) a co-non-dominant brain pattern, when both hemispheres are classified as *Non-Dominant*. Proportions of the four brain patterns were reported for the whole set, as well as separately for RH and LH individuals and for the Ambilateral and Strong-Atypical groups.

Language Production Induced-Activation of Brain Pattern Groups

To unravel the language production induced-activation at the basis of left-, right, co- dominance, and non-co-dominance, we performed a SPM group analysis on the four groups of brain pattern for language dominance. Then, we performed a second SPM analysis, testing whether the right-dominant group recruited brain regions homotopic to those of the left-dominant group (i.e., mirror-reversed organization) and/or whether the right-dominant group showed a different intra-hemispheric organization than the left-dominant group. Accordingly, we compared the BOLD contrast image of the left-dominant group to the left/right flipped (symmetrized with respect to the inter-hemispheric fissure in MNI stereotaxic space) BOLD contrast image of the right-dominant group. We performed (1) a conjunction analysis of the regional activation in the two contrast images (BOLD left-dominant and flipped BOLD right-dominant groups) for uncovering activations in homotopic regions, and (2) an analysis of regional activation differences between the two groups to reveal differences in intra-hemispheric organization. Significant foci of conjunction and differences are reported after applying a family-wise error (FWE) correction with $P < 0.05$.

RESULTS

RFE Procedure and Accuracy

The RFE accuracy curve that served as a basis for the selection of the best classifier is presented in Figure 3. We observed that classifier accuracy was situated above 95% for most of the procedure, with a sharp drop when less than 10 features were used. The classifier with the best accuracy was obtained at RFE iteration 25. Note that, as the three consecutive iterations (number 23, 24, and 25, Fig. 2) exhibited the same relative accuracy, we kept the most parsimonious classifier, namely that of iteration 25. This classifier used 789 of the initial 9,901 features (8%), and had a 97.6%. relative accuracy. The unbiased accuracy of the whole procedure was of 95.8%.

Map of Feature Weights (*W*) of the Winning Classifier

Location of the 789 features of the optimal classifier is displayed on Figure 4. This map contained positive (red) and negative (blue) weights (*W*) that will be involved in

the computation of the DV coding for the *Dominant* or *Non-Dominant* class. For example, *Dominant* class will include positive *W* associated with greater-than-average activity of the feature, or a negative *W* associated with a lower-than average activity, while the *Non-Dominant* class will include negative *W* associated with a greater-than-average activity, or positive *W* with a lower-than-average activity.

Positive weights were found in the frontal lobe and along the superior temporal sulcus (STS). In the frontal lobe, these clusters of positive features followed a dorso-ventral course along the anterior part of the precentral sulcus including spots at the junction of the precentral sulcus with the superior and the inferior frontal sulci, in the *pars opercularis* of the inferior frontal gyrus while others were located anteriorly in the *pars triangularis* of the inferior frontal gyrus, and at the anterior end of the horizontal branch of Sylvius in the *pars orbitaris* of the middle frontal gyrus. Medially, predictive clusters were found in the supplementary motor area (SMA). In posterior regions, predictive positive feature was located in the anterior parts and middle of the STS, and in the depth of STS ending corresponding to the angular gyrus. The putamen was also the site of positive feature location.

By contrast, negative weights were located in the ventral part of the anterior insula, in the anterior part of the inferior frontal gyrus and sulcus and in the anterior cingulate of the frontal lobe. Posteriorly they were found in the intraparietal sulcus, the posterior parts of STS at the junction with the occipital lobe, and in the inferior temporal gyrus. Finally, the caudate nucleus was a site of negative features weights.

Hemispheric SVM Predictions for the Learning Set

Using the SVM-RFE LOSO cross-validation procedure, 12 hemispheres were not classified as expected: six left-hemispheres were declared *Non-Dominant*, and six right-hemispheres were classified as *Dominant*. When considering the two hemispheres together, 238 individuals (95.2%) were considered as left-dominant, 6 (2.4%) as co-dominant (2 RH and 4 LH), and 6 (2.4%) as co-non-dominant (2 RH and 4 LH).

Hemispheric SVM Predictions for the Prediction Set

Among the 94 hemispheres of the prediction set, 53 hemispheres (56.3%) were classified as *Dominant* and 41 (43.6%) as *Non-Dominant*. The *Dominant* class was composed for 62.3% of left-hemispheres ($n = 33$), and for 37.7% of right-hemispheres ($n = 20$). The *Non-Dominant* classification was composed for 34.1% of left-hemispheres ($n = 14$) and for 65.8% of right-hemispheres ($n = 27$).

Note that the prediction using the final feature map of 280 features using the fivefold cross-validation method
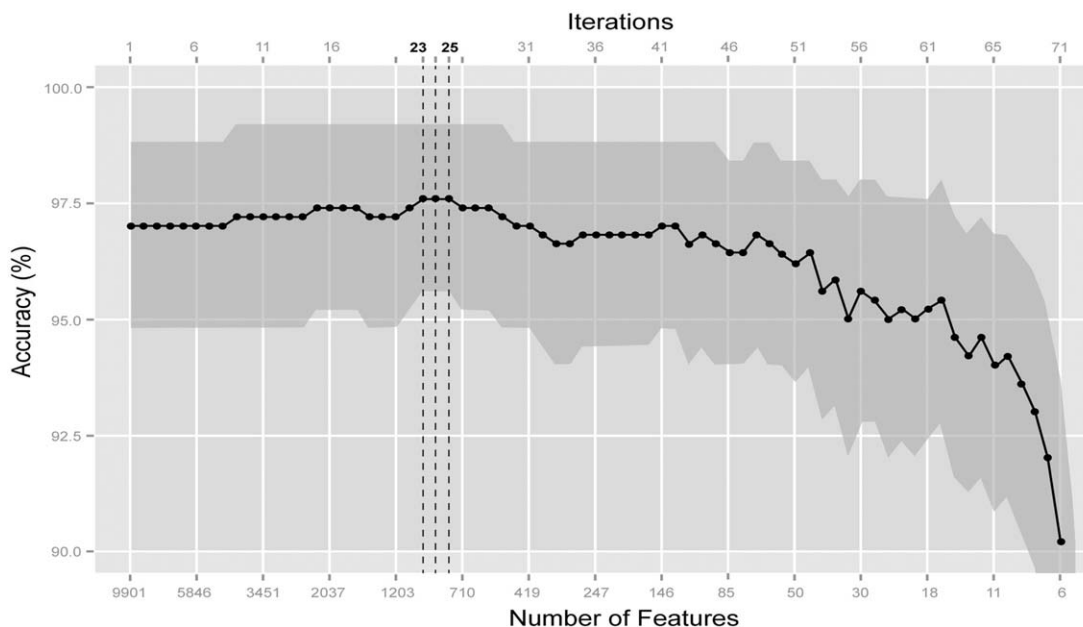
Figure 3.

Classifier accuracy against number of features at each iteration (the number of features is decreasing geometrically as a function of the iteration number). The best classifiers are obtained at iterations 23–25, with 789 features at least. The gray zone marks the approximate 90 % confidence interval around each accuracy value.

(see Supporting Information) was identical to LOSO, except in two participants that shifted from co-dominant to right-dominant (blue arrows, figure 3 in Supporting Information).

Brain Patterns of Language Dominance for the Prediction Set

When considering the two hemispheres together, occurrences of the 4 possible brain patterns of language dominance in the sample of 47 individuals of the prediction set were as follows (Table I): 51.1% were classified as left-dominant ($n = 24$), 23.4% as right-dominant ($n = 11$), 19.1% as co-dominant ($n = 9$), and 6.4% as co-non-dominant ($n = 3$). This distribution significantly differed from that observed in the learning set (Chi-square (3 d.o.f.) = 77.4, $P < 0.0001$).

Handedness

Splitting the sample by handedness, we found that a majority of non-typical RH (78.5%, 11 out 14) was classified as left-dominant with only 21.5% ($n = 3$) being co-dominant (Chi-square (1 d.o.f.) = 4.8, $P = 0.02$). No RH was found right-dominant or co-non-dominant. Note that all RH had a left-hemisphere classified as *dominant*.

By contrast, 39.4% of LH ($n = 13$) were classified as left-dominant, 33.3% ($n = 11$) as right-dominant, 18% ($n = 6$) as co-dominant and 9.0% ($n = 3$) as co-non-dominant. These distributions of brain patterns between RH and LH significantly differed (Chi-square (1 d.o.f.) = 8.2, $P = 0.04$).

HFLI groups

Splitting the sample by HFLI categories, we found that 64.8% of Ambilaterals had a left-dominant pattern ($n = 24$ out of 37), 21.6% ($n = 8$) were co-dominant, 8.1% were right-dominant ($n = 3$), and 5.4% were co-non-dominant ($n = 2$; Chi-square (3 d.o.f.) = 30.5, $P < 0.0001$). Note that, a large majority (72.9%) of individuals declared Ambilateral using the HFLI approach had actually a single (left or right) *dominant* hemisphere found by SVM.

Among the left-dominant individuals (11 RH and 13 LH, gray bars in Fig. 5A), it is noticeable that four were predicted to be left dominant despite very small DV absolute values for either their left (3 LH) or right (1 RH) hemisphere. The right-dominant class was composed of 3 LH only, including one with a small left hemisphere DV (Fig. 5B, green bars). The co-dominant class included three RH and five LH (Fig. 5B, purple bars), including one RH with a small right-hemisphere DV, and two LH with a small left hemisphere DV. Note that these LH with high right hemisphere DV and low left hemisphere DV are those that were classified right dominant applying the fivefold cross-validation procedure.

Finally, two LH Ambilaterals were classified as co-non-dominant with strong negative DV for both hemispheres (Fig. 5B, orange bars).
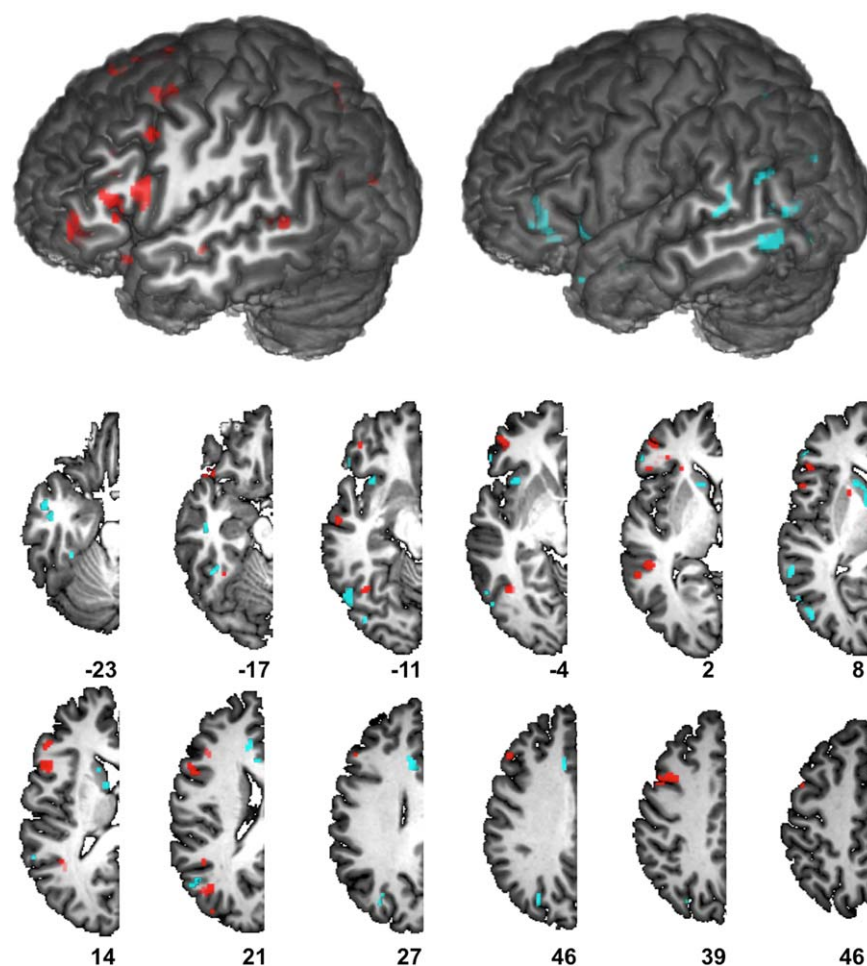
Figure 4.

Map of the positive (red) and negative (blue) feature weights (*W*) of the winning classifier superimposed onto an anatomical MRI image surface of one individual that served to define the 80-TVS template of the BIL&GIN. [Color figure can be viewed at wileyonlinelibrary.com]

Regarding Strong-Atypicals, 80% of them were classified as right-dominant ($n = 8$), 10% as co-dominant ($n = 1$), and 10% as co-non-dominant ($n = 1$). No strong-atypical individual was found left-dominant. As regards DV values (Table II and left side of Fig. 5B, green bars), one co-dominant individual showed large positive DV for his left and right hemispheres.

Language Production Induced Activation Patterns for SVM Classes

Left- or right-brain dominant groups

The class of individuals predicted to have a left-dominant brain pattern exhibited, as expected, larger extent of activation clusters in the left than in the right hemisphere in frontal language production areas including inferior frontal gyrus and sulcus, orbital frontal cortex,

and the junctions of the precentral sulcus with the superior and inferior frontal sulci. Posteriorly, STS was the site of activations, including a small anterior cluster and a large posterior one that extended to the occipito-parietal junction including the angular gyrus. Activations were also present in the posterior part of the inferior temporal gyrus. In the medial wall, increased activity was found in SMA extending to the middle cingulate gyrus and in the posterior cingulate gyrus extending to the precuneus. Subcortical activation was found in caudate nuclei (Table III and Fig. 6). In the right hemisphere of left-dominant brain pattern, almost symmetrical activations were present in the inferior frontal gyrus, STS and medial wall of the frontal gyrus.

The right-dominant brain pattern group was very close to the left-dominant group with activations in the right hemisphere mirroring those of the left hemisphere of left-dominant group. However, due to the smaller size of this

TABLE I. Percentages of individuals and hemispheric decision values (DV ± Standard deviation) are given for each brain dominance pattern category, and according to handedness (RH, LH) and HFLI (Ambilaterals, Strong-Atypicals) groups

	Left-dominant 51.1 (24)		Right-dominant 23.4 (11)		Co-dominant 19.1 (9)		Co-non-dominant 6.4 (3)	
	RH	LH	RH	LH	RH	LH	RH	LH
% subjects (n)	45.8 (11)	54.2 (13)	0	100 (11)	33.3 (3)	66.7 (6)	0	100 (3)
	Left-dominant		**Right-dominant**		**Co-dominant**		**Co-non-dominant**	
	RH	LH	RH	LH	RH	LH	RH	LH
Ambilateral (37)								
% subjects (n)	45.8 (11)	54.2 (13)	0	100 (11)	37.5 (3)	62.5 (5)	0	100 (2)
Left-Hem DV ± SD	+1.34 ± 0.91	+0.95 ± 0.46	/	−0.65 ± 0.55	+1.33 ± 0.69	+0.49 ± 0.93	/	−0.81 ± 0.71
Right-Hem DV ± SD	−1.25 ± 0.49	−0.97 ± 0.82	/	+0.76 ± 0.24	+0.59 ± 0.75	+0.93 ± 0.33	/	−0.53 ± 0.40
Strong-atypical (10)								
% subjects (n)	0	0	0	100 (8)	0	100 (1)	0	100 (1)
Left-Hem DV ± SD	/	/	/	−0.96 ± 0.80	/	+0.96	/	−1.01
Right-Hem DV ± SD	/	/	/	+1.46 ± 0.81	/	+0.61	/	−1.08

The numbers in parentheses correspond to the number of subjects.

group, activation extent was reduced, and in their left hemisphere only the *pars orbitaris* was the site of activation at the given statistical threshold.

Joint activation pattern in the dominant and non-dominant hemispheres for the left-dominant and right-dominant groups

Conjunction analysis revealed a pattern of brain areas jointly activated by both groups ($P < 0.05$ FWE) in their respective dominant and non-dominant hemispheres. As illustrated in Figure 6, this pattern included in the dominant hemisphere most of the above described frontal and STS activations, plus a site in the thalamus (Table III). In the non-dominant hemisphere, joint activation was only found in the *pars orbitaris* of the inferior frontal gyrus and in the posterior part of the cingulate gyrus.

The direct comparison of both contrasts did not reveal any significant difference in either hemisphere (dominant or non-dominant) between these groups ($P < 0.001$ uncorrected for multiple comparisons).

Co-dominant group

As illustrated in Figure 7, the group of nine co-dominant individuals showed bilateral increased activity during language production with a pattern very close to that of the left hemisphere of left dominant participants in both hemispheres.

Comparison of the co-dominant group to either left-dominant or right-dominant groups showed no significant difference ($P < 0.05$ FWE), indicating that co-dominant group did not involve additional specific intra-hemispheric activation during language production.

Co-non dominant group

As illustrated in Figure 7, the group of co-non-dominant individuals was characterized by activations involving more posterior areas. Left posterior activations were located in the inferior temporal and occipital gyri while on the right, they were seen at the posterior ending of STS, and at the occipito-temporal junction. In the left frontal lobe, the *pars orbitaris* and the junction between the middle frontal gyrus and precentral sulcus were significantly activated together with SMA. Activation of the posterior cingulate was present. The right frontal lobe activations were constituted of small clusters located in the superior frontal gyrus, within the *pars triangularis* and *pars orbitaris* of the inferior frontal gyrus, and at the junction of the inferior frontal sulcus with precentral sulcus. Finally, the right caudate was activated.

DISCUSSION

Methodological Issues

The SVM approach we have implemented allowed us characterizing language hemispheric dominance and its
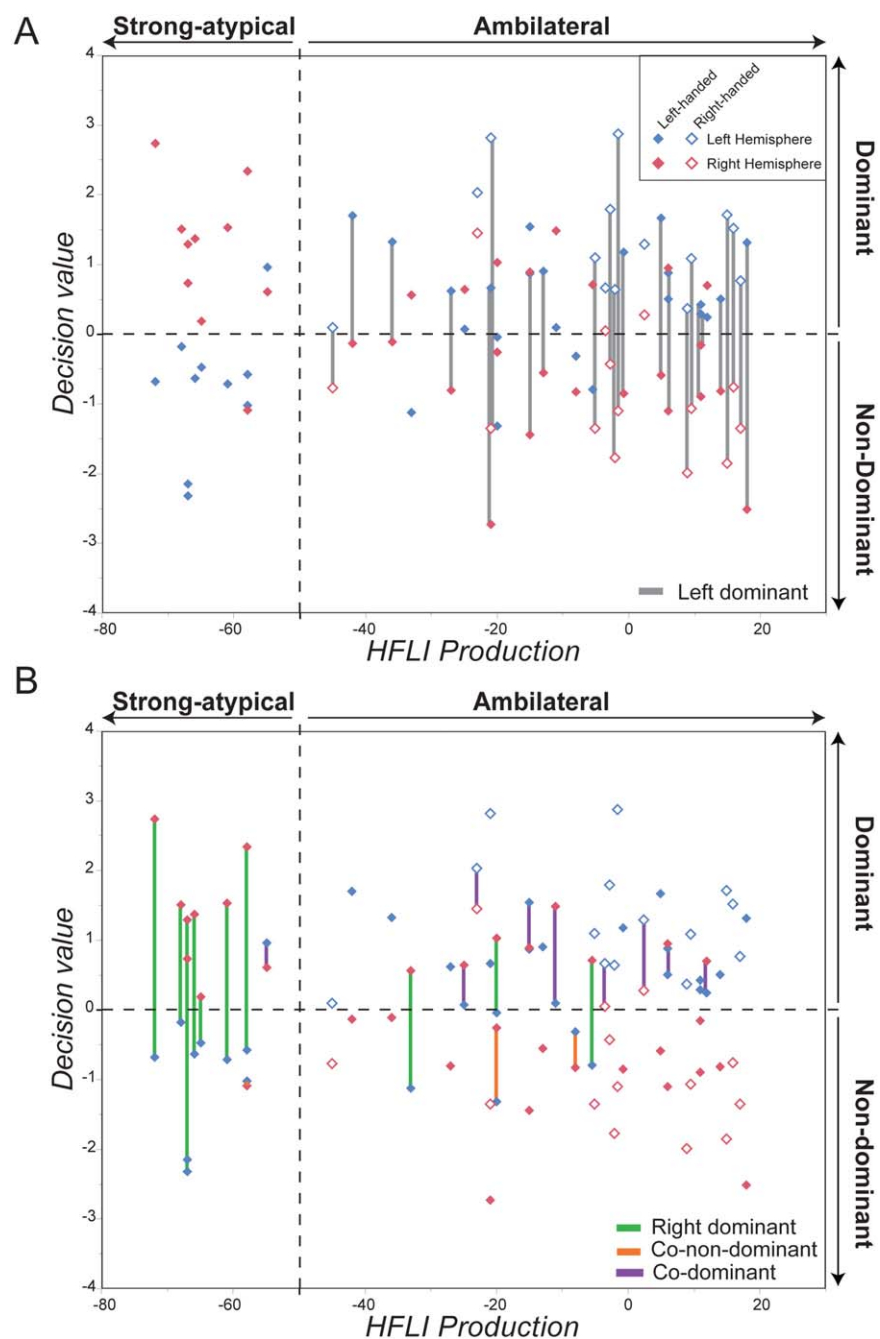
Figure 5.

Decision value of each hemisphere of the prediction set in function of the hemispheric functional lateralization index (HFLI) for language production. Positive and negative decision values code for Dominant/Non-Dominant hemispheres, respectively. Based on the HFLI analysis, subjects were classified as Strong- Atypical (HFLI < −50) or Ambilateral (HFLI >= 50) [Mazoyer et al., 2014]. (**A**) Each left-dominant individual is highlighted with a vertical line joining its two hemispheres (gray line). (**B**) Each right-dominant (green line)/co-non-dominant (orange line)/ co-dominant (purple line) subject is highlighted with a vertical line joining its two hemispheres. [Color figure can be viewed at wileyonlinelibrary.com]

TABLE II. Summary table for the SPM group analysis

N voxels	Anatomical localization	Peak voxel (MNI coordinates)			T score
		x	y	z	
Left-dominant group (N = 24)					
Left hemisphere					
2896	Inf frontal gyrus, pars triangularis	−46	18	22	11.5
	Mid frontal gyrus, pars orbitaris	−42	30	−12	7.3
3367	Fusiform gyrus	−40	−54	−16	10.7
	Mid occipital gyrus	−44	−66	26	8.6
3089	Supp Motor Area (SMA)	−4	14	64	10.3
403	Precuneus/post cingulate gyrus	−2	−52	10	8.1
352	Caudate	−10	−8	8	8.9
25	Sup frontal sulcus	−18	12	40	6.8
59	Mid temporal gyrus	−60	−4	−10	6.4
47	Precuneus	−4	−56	40	6.3
Right hemisphere					
2077	Fusiform gyrus	40	−52	−14	11.0
	Mid occipital gyrus	44	−64	22	9.4
612	Inf inferior frontal sulcus	58	34	0	9.5
	Mid frontal gyrus, pars orbitaris	40	36	−14	9.3
169	Mid temporal gyrus	58	−6	−16	7.0
21	Sup frontal gyrus, pars orbitaris	4	32	−20	6.8
49	Inf frontal gyrus, pars triangularis	38	14	26	6.7
Right-dominant (N = 11)					
Left hemisphere					
20	Inf frontal gyrus, pars orbitaris	−52	28	−6	6.0
Right hemisphere					
1366	Inf frontal gyrus, pars orbitaris	52	32	0	10.6
	Inf frontal gyrus (Tri)	40	14	26	8.7
	Precentral sulcus	48	10	44	8.0
728	SMA	10	12	62	9.9
239	Mid frontal gyrus, pars orbitaris	36	38	−12	8.4
68	Inf occipital gyrus	50	−46	2	7.8
100	Precuneus/post cingulate gyrus	0	−52	12	7.8
194	Mid temporal gyrus	46	−60	16	7.7
117	Caudate	10	−6	8	7.5
21	Thalamus	20	2	4	6.1
Co-dominant (N = 9)					
Left hemisphere					
68	Caudate	−18	8	12	7.4
190	Med sup frontal gyrus	−2	34	34	6.9
67	Mid frontal gyrus, pars orbitaris	−42	30	−12	6.8
26	Ant insula	−32	16	−4	6.7
183	Inf frontal sulcus	−52	36	8	6.7
46	Mid temporal gyrus	−60	−46	2	6.6
Right hemisphere					
47	Mid frontal gyrus, pars orbitaris	36	38	−12	8.0
376	SMA	2	12	66	7.8
116	Inf frontal gyrus, pars orbitaris	52	32	0	7.4
34	Sup temporal sulcus	50	−34	0	6.5
95	Precentral sulcus	44	6	40	6.5
20	Ant insula	36	16	−4	6.3
Co-non-dominant (N = 3)					
Left hemisphere					
72	Sup temporal sulcus	−56	16	−32	5.0
186	SMA	−2	18	54	4.8
113	Lat occipital gyrus	−38	−96	6	4.3
114	Mid temporal gyrus	−50	−68	−6	4.0
Right hemisphere					
394	Cingulate sulcus	6	28	38	5.6
197	Mid cingulate gyrus	6	−4	20	5.4
250	Ant cingulate gyrus	2	28	10	4.7
187	Inf temporal gyrus	50	−70	−4	4.6
89	Thalamus	16	−30	2	4.5
348	Ant insula	50	22	2	4.5
72	Sup frontal gyrus	16	18	70	4.2
112	Sup frontal sulcus	10	50	38	4.2

Each comparison is thresholded at $P < 0.05$ FWE except for the co-non-dominant group, which was reported at $P < 0.001$ uncorrected for multiple comparisons at the cluster level due to the low number of subjects.

TABLE III. Summary table for the conjunction analysis between BOLD left-dominant group and flipped BOLD right-dominant group (P < 0.05 FWE)

N voxels	Anatomical localization	Peak voxel (MNI coordinates)			T score
		x	y	z	
Dominant hemisphere					
624	SMA	−10	14	64	8.8
72	Ant cingulate	−8	26	28	5.8
1400	Inf frontal gyrus, pars orbitaris	−52	32	2	8.0
	Precentral sulcus	−54	18	18	6.8
	Mid frontal gyrus	−46	6	46	6.6
71	Thalamus	−10	−8	8	6.8
157	Mid temporal gyrus	−46	−62	18	6.6
29	Sup temporal gyrus	−48	−48	2	6.1
Non-dominant hemisphere					
49	Inf frontal gyrus, pars orbitaris	52	30	−4	6.8
26	Post cingulate	0	−54	10	5.9

This analysis was performed to evidence conjoint brain regions of the dominant hemisphere (corresponding to left hemisphere for left-dominant group, and to right hemisphere for the right-dominant group) and of the non-dominant hemisphere (corresponding to the right hemisphere for the left-dominant group and to the left hemisphere for the right-dominant group).

variability in healthy individuals. Specifically, in individuals showing non-typical HLI, SVM was able to assess the *dominant* or *non-dominant* type of each hemisphere activation pattern during language production, and explore whether individuals with non-typical lateralization as defined from asymmetry in hemispheric activity during the task are different in terms of their intra-intra-hemispheric organization of language networks. Actually, the SVM approach, different from the activation asymmetry measures, does not rely only on difference across hemispheres in the magnitude of activation, but mainly rely on the topographical organization of activations in a given hemisphere. Such a classification cannot be derived from the sole comparison of activations in one hemisphere relative to the other one, as it is done when computing hemispheric laterality index, or regional asymmetry. Rather, the unique strength of the SVM approach is that it gives information on the dominance and/or non-dominance of the activation pattern of one hemisphere, independently of the other for each individual.

This SVM hemisphere classification made on the learning set showed that 2.4% of the hemispheres of the learning set was potentially wrongly classified according to the HFLI typical language lateralized categorization. In the learning set, which we recall was exclusively composed of individuals with strong leftward asymmetry, we found that 12 hemispheres belonging to 12 different individuals (including 8 LH) were "wrongly" classified. Six of these individuals had a right hemisphere classified as *Dominant*,

leading to a co-dominant brain pattern. Meanwhile, for six other individuals, the left-hemisphere was classified as *Non-Dominant*, leading to co-non-dominant brain pattern.
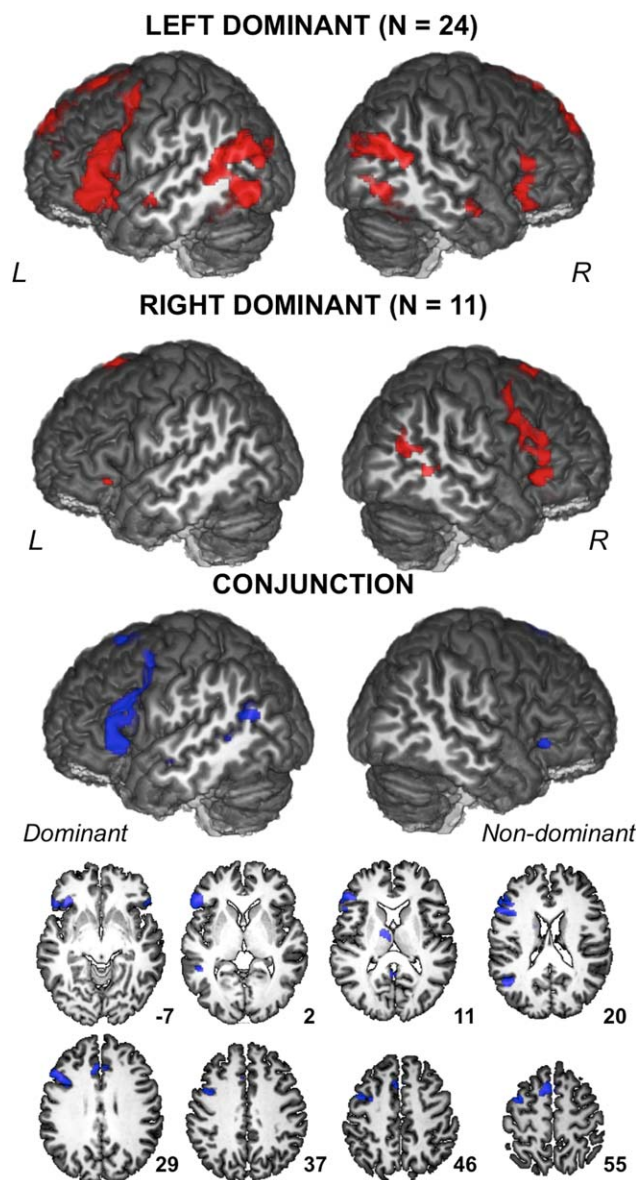

Figure 6.

Three-dimensional rendering of the statistical parametric maps of sentence production minus the recitation of a list of words activations in the left-dominant and right-dominant SVM groups. The conjunction analysis between BOLD left-dominant group and flipped BOLD right-dominant group revealed the brain regions that are conjointly activated in the dominant hemisphere and the non-dominant hemisphere of each group. Displayed results are significant at P < 0.05 with family-wise error (FWE) rate correction for multiple comparisons (R right; L left), and superimposed onto an anatomical MRI image surface of one individual that served to define the 80-TVS template of the BIL&GIN. [Color figure can be viewed at wileyonlinelibrary.com]
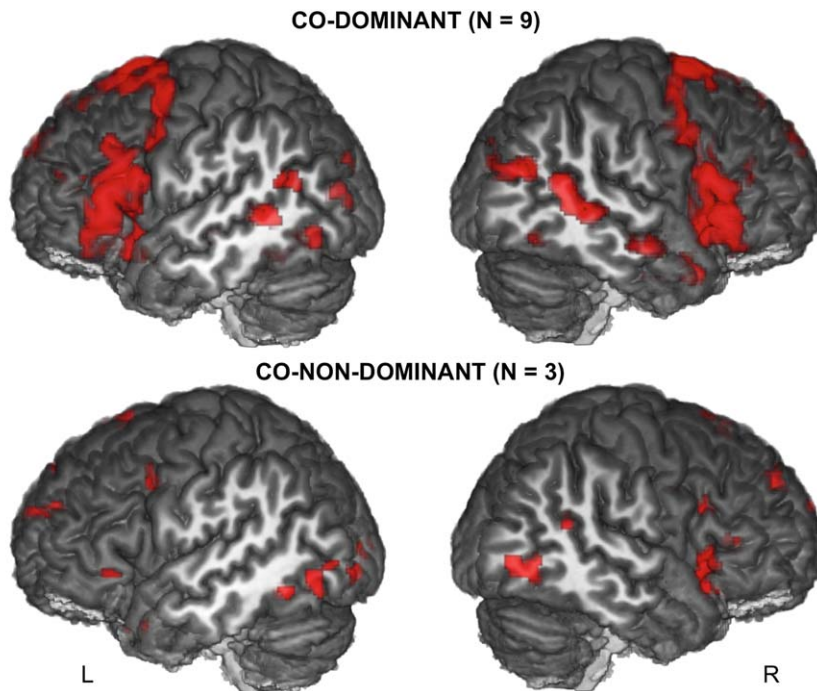
CO-DOMINANT (N = 9)

CO-NON-DOMINANT (N = 3)

L   R

Figure 7.

Three-dimensional rendering of the statistical parametric maps of sentence production minus the recitation of a list of words activations in the co-dominant and co-non-dominant SVM groups. Results are displayed at $P < 0.001$ uncorrected for multiple comparisons and superimposed onto an anatomical MRI image surface of one individual that served to define the 80-TVS template of the BIL&GIN (L: left; R: right). [Color figure can be viewed at wileyonlinelibrary.com]

No right-dominant pattern was found. Strikingly, the inspection of the contrast maps of these subjects revealed that the SVM procedure did actually work correctly. For example, as illustrated in Figure 8, one of the co-dominant individuals exhibited strong right hemisphere activations in language production areas, albeit of smaller amplitudes than their left hemispheric homotopic counterparts: their presence logically led the SVM classifier at correctly declaring the right-hemisphere as *dominant*. For the co-non-dominant individuals, here again, the SVM classifier correctly declared these hemispheres to be of the non-dominant type, as shown in Figure 8, the co-non-dominant individual showed bilateral posterior activation. Overall, these so-called errors exemplify the superiority of a voxel-based SVM classifier over the HFLI approach for assessing hemispheric specialization, the latter approach relying only on the asymmetry of the hemispheric activation patterns.

A limitation of SVM is that it necessitates the normalization of individuals' activation strength, thereby not considering the quantitative difference in activation across hemispheres contrasting with what the HFLI or any asymmetry index does. In other words, while an asymmetry index provides a quantitative difference in neural activity of one hemisphere relatively to the other at low spatial resolution (hemispheric or regional), SVM provides differences in hemispheric pattern, at a voxel-wise resolution. As we will see later, while SVM provides clear categorization when HFLI is unable to discriminate hemispheres, HFLI can be complementary to SVM in case of co-dominance to reveal the most recruited hemisphere. Combined, the two methods are likely to provide an accurate tool for determination of the language dominance pattern of a given individual.

Hemispheric Classification

A first original finding is that, in a group of 47 individuals previously labeled as non-typical for language lateralization using an index of hemispheric functional asymmetry, at least one hemisphere was found to be dominant using a SVM approach in every but three individuals, indicating that the "dominant" type of functional organization is by and large the most frequent. Indeed, correcting for the LH enrichment of our sample and assuming a 10% prevalence of LH in the population, one can estimate the frequency in non-typicals individuals of having at least one hemisphere of the *dominant* type to be on the order of 98%. Faced with such an overwhelming prevalence, one may hypothesize that the hemispheric dominance, as defined with SVM, is biologically pre-programmed, being a sort of "default
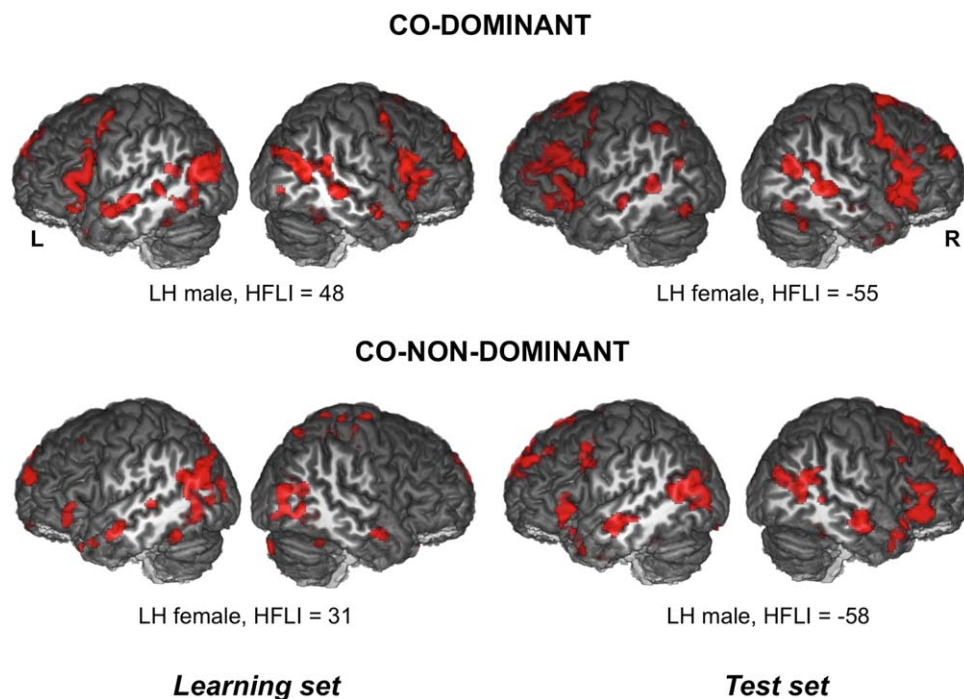
CO-DOMINANT

LH male, HFLI = 48   LH female, HFLI = -55

CO-NON-DOMINANT

LH female, HFLI = 31   LH male, HFLI = -58

Learning set   *Test set*

Figure 8.

Three-dimensional rendering of the statistical parametric maps of sentence production minus the recitation of a list of words activations (*P* = 0.001 uncorrected for multiple comparisons for illustrative purpose) of four individuals with one of their hemisphere "wrongly" classified with the SVM classifier according to the HFLI value. Learning set: one individual is classified as co-dominant (HFLI = +48) and the other is classified as co-non-dominant (HFLI = +31). Prediction set: one individual is classified as co-dominant (HFLI = −55) and the other is classified as co-non-dominant (HFLI = −58). Displayed results are significant at *P* < 0.001 uncorrected for multiple comparisons and superimposed onto an anatomical MRI image surface of one individual that served to define the 80-TVS template of the BIL&GIN (R: right; L: left). [Color figure can be viewed at wileyonlinelibrary.com]

mode" hemispheric organization for language that can be observed in both hemispheres.

A second important finding is that the left hemisphere is classified as *dominant* in the majority of non-typical individuals' cases, including 100% of RH and 57.4% of LH. This latter difference is mainly due to the fact that the LH non-typical group gathered Strong-Atypical individuals who exhibited a right dominant hemisphere. Correcting again for the sample LH enrichment, we estimated the frequency of a dominant left-hemisphere in non-typicals to be 90%. This figure is important because it shows that left hemisphere remains the most likely one to support language production functions even in healthy non-typical individuals.

More Variability of the Brain Patterns of Language Dominance in LH

In non-typical individuals, the brain pattern most frequently predicted (51.1%) was the typical left-dominant one, and it concerned exclusively individuals with weak cerebral lateralization who were categorized as Ambilaterals in Mazoyer et al.' study [2014]. This finding demonstrates that, even in case of weak asymmetry, the typical *left hemisphere dominant* organizational pattern remains the most frequent one. Coherently, voxel-based analysis in these 24 individuals exhibited involvement of the typical fronto-temporal language network [Tzourio-Mazoyer et al., 2016; Vigneau et al., 2006], with larger activation in the left than in the right hemisphere.

When considering handedness, we observed that not only all RH had a dominant hemisphere, but also that almost 80% of them had a left-dominant pattern, a finding consistent with the fact that the regional profiles of asymmetry of the right-handed Ambilateral group was strongly correlated with that of the Typical group [Tzourio-Mazoyer et al., 2016]. On the opposite, LH Ambilaterals, taken as a group, had a profile of regional asymmetries different from other categories. The present work provides a possible explanation for this observation: indeed, a huge variability was observed among left-handed Ambilaterals among whom the four types of brain lateralization patterns were present. This demonstrates that in cases where HFLI cannot provide clear-cut information on the

dominant hemisphere of a given individual (or if any), SVM offers the possibility of a characterization. However, as it will be further developed, a combination of the two approaches might still be valuable in cases of co-dominance when one wants to estimate what is the most important hemisphere for language processing.

Finally, although by design, SVM could predict 4 brain patterns only, one should consider association of co-dominance or co-non-dominance with a strong HFLI as additional brain dominance patterns. Actually, we observed both leftward asymmetrical co-dominant individuals within the learning set of Typicals and rightward asymmetrical co-dominant individuals within Strong-atypicals in the prediction set, what might indicate the existence of two additional brain dominance patterns. In the same vein, we also observed leftward asymmetrical co-non-dominant individuals in the learning set of Typicals and rightward asymmetrical co-non-dominant individuals in the prediction set, indicating again two more dominance patterns. Notably, these four additional brain patterns represent very rare variant patterns in the general population.

Same Intra-Hemispheric Organization for Right-Dominant and Left-Dominant Individuals

The second most frequent brain dominance pattern in non-typically lateralized individuals was the right-dominant pattern (around 23% of the prediction set). This group of 11 individuals is likely to correspond to individuals exhibiting speech arrest after right intracarotid amobarbital injection during WADA test such as observed in epileptic patients [Benbadis et al., 1995; Möddel et al., 2009; Rasmussen and Milner, 1977]. In healthy participants, a right-dominant pattern has been also found with fTCD [Knecht et al., 2000]. Interestingly, all these 11 right-dominant participants were LH, thereby reinforcing the hypothesis that reverse language hemispheric organization can only be observed in LH. Furthermore, eight of these eleven right-dominant brain pattern individuals showed strong rightward HFLI values and corresponded to individuals included in the Strong-Atypical group [Mazoyer et al., 2014]. This indicates that individuals exhibiting a strong rightward lateralization are preferentially those showing right-dominant language organization and that in 80% of the cases (8 out of 10 Strong-atypicals), a strong rightward hemispheric asymmetry truly corresponds to a right hemisphere having a dominant pattern. For the 20% remaining, one individual was predicted to be co-dominant, and the other was co-non-dominant. For the co-dominant Strong-atypical individual, the fact that the predictive DVs were comparable across hemispheres and that the HFLI asymmetry index was equal to −55 (i.e., very strongly rightward) questions the role of each hemisphere during the language production task in this peculiar participant. One may propose that if both hemispheres have a dominant pattern but with lower activation on the left, the

right hemisphere shows more activation, and becomes more lateralized. However, there is currently no non-invasive way to answer this question, although the examination of the individual pattern of activation illustrated on Figure 7 confirms the stronger involvement of the right hemisphere, consistent with HFLI negative value. One perspective of this study would be to consider both SVM and HFLI approaches when evaluating individual dominance. Further studies using the confrontation with Wada testing are needed in patients having such a profile to test the hypothesis that speech arrest would be obtained after anesthesia of either hemisphere, but would be more severe when the right one is disabled.

The group analysis of the 11 right-dominant individuals clearly demonstrated that their brain pattern mirrors the left-dominant one, as the conjunction of the two groups showed identical pattern of activation and group comparison did not highlight any significant difference. These findings indicated that the pattern of regional activations of the dominant hemisphere corresponds to the "classical" language network, including inferior frontal and precentral regions as well as the posterior part of the STS. This is also consistent with the negative correlation that was found within the regional asymmetries between Strong-atypicals (right-lateralized LI) and Typicals (left-lateralized LI) groups [Tzourio-Mazoyer et al., 2016]. In addition, the intra-hemispheric SVM approach evidenced conjoint activation in the non-dominant hemisphere, in particular within the orbital part of the inferior frontal gyrus. Although the functional role of this area within the non-dominant hemisphere needs to be clarified, maybe related to attentional/executive processes involved in the task [Aron et al., 2004], these results emphasized the fact that the frontal lobe is decomposed into a mosaic of different regions according to the dominant or non-dominant hemispheric role in a given function.

Finally, consistent with the study of Chang et al. [2011] of a homotopic organization of essential language sites, one may conclude that the right-dominant individuals have the same intra-hemispheric language organization that the left-dominant ones, the only change being the side of the activations.

Rare Co-Dominant and Co-Non-Dominant Brain Patterns Can Be Observed in Healthy Individuals

The SVM approach we used demonstrated that in healthy individuals both co-dominance and co-non-dominance brain patterns exist and should thus be considered as normal variants of hemispheric specialization and are not mandatory related to the presence of an epileptogenic lesion [Tzourio-Mazoyer et al., 2017]. Co-dominance was rare (15 participants including 12 LH when accounting for the 6 LH of the learning set), its occurrence being estimated at 5% in the population, affecting mostly LH. The proportion of co-dominant is even lower when

considering the classification provided with the fivefold-based method as two co-dominant LH were classified as right dominant with this last method. In 445 epileptic patients explored with Wada testing, Möddel reported 6% of patients with bilateral dependent hemispheres corresponding to speech arrest elicited during anesthesia of either hemisphere [Möddel et al., 2009]. This could likely correspond to the co-dominance observed in our study. Occurrence of co-dominance seems thus of similar amplitude in epileptics and in healthy individuals, although concerning a larger proportion of LH in the latter group (73%) than in the patient group (21%). This hypothesis of more balanced hemispheric dominance in LH is consistent with recent results from a repetitive navigated transcranial magnetic stimulation study that demonstrated that LH present a comparatively equal language distribution across both hemispheres with language dominance being nearly equally distributed between hemispheres in contrast to RH [Tussis et al., 2016]. One may thus consider that co-dominance is a variant of brain pattern of language dominance that can be seen in healthy subjects, although more frequently in those having an atypical unimanual gestures lateralization. Examination of the regional activation pattern of the nine co-dominant participants demonstrated the recruitment of frontal and temporal areas comparable—although in both hemispheres—to what was seen in the left hemisphere of typical individuals. These subjects are thus likely representative of the ambilaterals described by Hécaen, who showed aphasia after either hemisphere lesion with an evolution marked by very good recovery [Hécaen et al., 1981].

Finally, co-non-dominance was the most striking pattern. It was very rare (9 individuals out of 297, including 7 LH, 3% of our sample). It must be underlined that the DVs for these three subjects of the prediction set were not lower than those observed in other groups, meaning that there was no ambiguity regarding the prediction of the two hemispheres as *non-dominant*. The proportion reported here in healthy individuals is different to that reported in epileptics, if one considers that the co-non-dominant pattern we reported can be matched to that of patients showing no speech arrest after anesthesia of either hemisphere, labeled as "bilateral-independent" in Möddel et al.' study [2009]. Among 445 epileptic patients, 9% of them are found to be "bilateral-independent" with a higher occurrence of LH (25%) compared with the proportion of LH in the left-dominant group (7%) [Möddel et al., 2009]. These findings indicate that this kind of hemispheric organization appears to be an option observed when plasticity mechanisms occur, and although rare, co-non-dominance is a normal variant of language dominance in healthy LH individuals. These observations are in line with Price' proposal of degeneracy, suggesting that reorganization occurs along paths that can be revealed by inter-individual variability patterns as observed in healthy individuals [Price and Friston, 2002]. Although a precise evaluation of this non-dominant pattern is difficult due to their very small prevalence, language networks of these participants appeared to be different from that of typicals in terms of recruited areas. While the group analysis on these three individuals pointed to the involvement of posterior occipito-temporal regions that were shown to pertain to the negative features map, the individual analysis illustrated in Figure 8 showed activation in other frontal and temporal regions. These findings that co-non-dominance pattern corresponds to a very peculiar intra-hemispheric organization, that certainly required further investigations.

CONCLUSION

The use of SVM allowed us to progress in the understanding of the intra- and inter-hemispheric organization of language production in healthy individuals considered as non-typical. By providing the *dominant/non-dominant* character of each hemisphere in each individual, this approach allowed discriminating among participants showing weak asymmetry, those having a dominant hemisphere from the rare ones having two *dominant* or two *non-dominant* hemispheres. Although it does not take into account quantitative differences in activation across hemispheres, a complementary information that may be provided by asymmetry indices in case of co-dominance, such SVM classifier opens the way to further investigations in patients within the framework of pre-surgical mapping to confront such classification to that of the Wada testing, still considered as the gold standard.

ACKNOWLEDGMENT

REFERENCES

Ambroise C, McLachlan GJ (2002): Selection bias in gene extraction on the basis of microarray gene-expression data. Proc Natl Acad Sci USA 99:6562–6566.

Aron AR, Robbins TW, Poldrack RA (2004): Inhibition and the right inferior frontal cortex. Trends Cogn Neurosci 8:170–177.

Baciu M, Juphard A, Cousin E, Le Bas J-F (2005a): Evaluating fMRI methods for assessing language dominance in healthy subjects. Eur J Radiol 55:209–218.

Baciu MV, Watson JM, Maccotta L, McDermott KB, Buckner RL, Gilliam FG, Ojemann JG (2005b): Evaluating functional MRI procedures for assessing hemispheric language dominance in neurosurgical patients. Neuroradiology 47:835–844.

Benbadis SR, Dinner DS, Chelune GJ, Piedmonte M, Lüders HO (1995): Objective criteria for reporting language dominance by intracarotid amobarbital procedure. J Clin Exp Neuropsychol 17:682–690.

Benke T, Köylü B, Visani P, Karner E, Brenneis C, Bartha L, Trinka E, Trieb T, Felber S, Bauer G, Chemelli A, Willmes K (2006): Language lateralization in temporal lobe epilepsy: A

comparison between fMRI and the Wada test. Epilepsia 47: 1308–1319.

Binder JR (2011): Functional MRI is a valid noninvasive alternative to Wada testing. Epilepsy Behav 20:214–222.

Chang EF, Wang DD, Perry DW, Barbaro NM, Berger MS (2011): Homotopic organization of essential language sites in right and bilateral cerebral hemi-spheric dominance. J Neurosurg 114:893–902.

Chen P, Lin C, Schölkopf B (2005): A tutorial on v-support vector machines. Appl Stoch Models Bus Ind 21:111–136.

Drane DL, Roraback-Carson J, Hebb AO, Hersonskey T, Lucas T, Ojemann GA, Lettich E, Silbergeld DL, Miller JW, Ojemann JG (2012): Cortical stimulation mapping and wada results demonstrate a normal variant of right hemisphere language organization. Epilepsia 53:1790–1798.

Dym RJ, Burns J, Freeman K, Lipton ML (2011): Is functional MR imaging assessment of hemispheric language dominance as good as the Wada test?: A meta-analysis. Radiology 261:446–455.

Guyon I, Weston J, Barnhill S, Vapnik V (2002): Gene selection for cancer classification using support vector machines. Mach Learn 46:389–422.

Hécaen H, De Agostini M, Monzon-Montes A (1981): Cerebral organization in left-handers. Brain Lang 12:261–284.

Joliot M, Jobard G, Naveau M, Delcroix N, Petit L, Zago L, Crivello F, Mellet E, Mazoyer B, Tzourio-Mazoyer N (2015): AICHA: An atlas of intrinsic connectivity of homotopic areas. J Neurosci Methods 254:46–59.

Knecht S, Dräger B, Deppe M, Bobe L, Lohmann H, Flöel A, Ringelstein EB, Henningsen H (2000): Handedness and hemispheric language dominance in healthy humans. Brain 123: 2512–2518.

Mazoyer B, Zago L, Jobard G, Crivello F, Joliot M, Perchey G, Mellet E1, Petit L, Tzourio-Mazoyer N (2014): Gaussian mixture modeling of hemispheric lateralization for language in a large sample of healthy individuals balanced for handedness. PLoS One 9:e101165.

Mazoyer B, Mellet E, Perchey G, Zago L, Crivello F, Jobard G, Delcroix N, Vigneau M, Leroux G, Petit L, Joliot M, Tzourio-Mazoyer N (2015): BIL&GIN: A neuroimaging, cognitive, behavioral, and genetic database for the study of human brain lateralization. NeuroImage 124:1225–1231.

Möddel G, Lineweaver T, Schuele SU, Reinholz J, Loddenkemper T (2009): Atypical language lateralization in epilepsy patients. Epilepsia 50:1505–1516.

Noble WS (2006): What is a support vector machine? Nat Biotechnol 24:1565–1567.

Oldfield RC (1971): The assessment and analysis of handedness: The Edinburgh inventory. Neuropsychologia 9:97–113.

Price CJ, Friston KJ (2002): Degeneracy and cognitive anatomy. Trends Cogn Sci 6:416–421.

Rasmussen T, Milner B (1977): The role of early left-brain injury in determining lateralization of cerebral speech functions. Ann N Y Acad Sci 299:355–369.

Schölkopf B, Smola AJ, Williamson RC, Bartlett PL (2000): New support vector algorithms. Neural Comput 12:1207–1245.

Seghier ML, Kherif F, Josse G, Price CJ (2010): Regional and hemispheric determinants of language laterality: Implications for preoperative fMRI. Hum Brain Mapp 32: 1602–1614.

Tussis L, Sollmann N, Boeckh-Behrens T, Meyer B, Krieg SM (2016): Language function distribution on left-handers: A navigated transcranial mangetic stimulation study. Neuropsychologia 82:65–73.

Tzourio-Mazoyer N, Joliot M, Marie D, Mazoyer B (2016): Variation in homotopic areas' activity and inter-hemispheric intrinsic connectivity with type of language lateralization: an fMRI study of covert sentence generation in 297 healthy volunteers. Brain Struct Funct 221:2735–2753.

Tzourio-Mazoyer N, Perrone-Bertolotti M, Jobard G, Mazoyer B, Baciu M (2017): Multi-factorial modulation of hemispheric specialization and plasticity for language in healthy and pathological conditions: A review. Cortex 86:314–339.

Vigneau M, Beaucousin V, Hervé PY, Duffau H, Crivello F, Houdé O, Mazoyer B, Tzourio-Mazoyer N (2006): Meta-analyzing left hemisphere language areas: Phonology, semantics, and sentence processing. NeuroImage 30:1414–1432.

Wilke M, Schmithorst VJ (2006): A combined bootstrap/histogram analysis approach for computing a lateralization index from neuroimaging data. NeuroImage 33:522–530.